Lipid-protein interactions in mitochondrial membranes from bivalve mollusks: molecular strategies in different species

Lipid-protein interactions in mitochondrial membranes from bivalve mollusks: molecular strategies in different species

Rosamaria Fiorini[a], Vittoria Ventrella[b], Fabiana Trombetti[b], Micaela Fabbri[b], Alessandra Pagliarani[b], Salvatore Nesci[b]

[a]Department of Life and Environmental Sciences, Marche Polytechnic University, Montedago, 60131 Ancona, Italy

[b]Department of Veterinary Medical Sciences, University of Bologna, 40064 Ozzano Emilia, Bologna, Italy

Corresponding author: Alessandra Pagliarani alessandra.pagliarani@unibo.it

Abstract

In spite of commonalities in the rotary mechanism of the mitochondrial F_1F_O-ATPase, the key enzyme in cell bioenergetics, our previous studies on mussel gill mitochondrial membranes pointed out a raft-like arrangement, which apparently distinguishes bivalve mollusks from mammals. On these bases, the physico-chemical features of mitochondrial membranes and the F_1F_O-ATPase activity temperature-dependence are here explored in the Manila clam (*Ruditapes philippinarum*), of known adaptive success and environmental tolerance. Similarly to the mussel, clam gill mitochondrial membrane lipids exhibit a high sterol content (42 mg/g protein), mainly due to phytosterols (cholesterol only attains 42% of total sterols), and abundant polyunsaturated fatty acids (PUFA) (70% of total fatty acids), especially of the n-3 family. However, the F_1F_O–ATPase activation energies above and below the break in the Arrhenius plot (22.1 °C) are lower than in mussel and mammalian mitochondria. Laurdan fluorescence spectroscopy analyses carried out at 10°, 20° and 30°C on mitochondrial membranes and on liposomes obtained from total lipid extracts of mitochondria, indicate a physical state without coexisting domains. This mitochondrial membrane texture, allowed by lipid-lipid and lipid protein interactions and involving PUFA-rich phospholipids, phytosterols (much more diversified in clams than in mussels) and proteins, allows the maintenance of a homogeneous physical state in the range 10-30°C. Consistently, this molecular interaction network would somehow extend the temperature range of the F_1F_O–ATPase activity and contribute to clam resilience to temperature changes.

Key words: Manila clam; mitochondrial F_1F_O-ATPase; Laurdan fluorescence; temperature dependence; sterols; polyunsaturated fatty acids

1. Introduction

From a biochemical standpoint, the molecular interactions among biomolecules address and rule the biological properties of organisms and contribute to determine their lifestyle. Accordingly, the structure of biomembranes and the interactions among structural membrane components are essential for cell life and organism adaptation to the environment (Los and Murata, 2004). Intriguingly, the molecular texture of biological membranes which host and modulate enzyme complexes of outstanding role in bioenergetics may even hide the key of the different survival extent and adaptation capability of animal species to changing environmental conditions. Marine poikilotherms, and especially bivalve mollusks, sessile or endowed with a limited motility, are expecially prone to environmental challenges and changes, especially if they live in shallow waters, typical of intertidal and subtidal habitats, which normally undergo environmental fluctuations of physico-chemical conditions. With this hypothesis in mind, we focused on mitochondrial membranes, being the mitochondrion the well known powerhouse of eukaryotic cells. Lipid-protein interactions, of main relevance in the inner mitochondrial membrane which hosts the bioenergetic enzyme machinery, build a complex network, which contributes to the membrane physical state and rules membrane-bound enzyme functions, other than the access of modulators which directly intervene on the enzymes. Moreover, the recent technologies lead to decipher wider roles of lipid-protein interactions, which seem to complement and even overwhelm the classical ones (Saliba et al., 2015). Fatty acids and sterols are among the key molecules which maintain membranes in a state of fluidity adequate for function. Accordingly, eukaryotic mitochondria exhibit a quite similar phospholipid composition. Phospholipid heads influence the proportion between planar bilayer and hexagonal phase formation (Mejia and Hatch, 2016). Even if the ratio of bilayer stabilizing to destabilizing phosphospholipids is involved in temperature acclimation of poikilotherms, no change was found in mitochondria from bivalve mollusks acclimated to different temperatures (Gills and Ballantyne, 1999). On the other hand the interplay between saturated and unsaturated

fatty acids is long known to be crucial in membrane homeoviscous adaptation (Ernst et al., 2016), but in recent years sterols emerge as critical components for the formation of liquid-ordered membrane states, the so-called lipid rafts, which play a role in membrane dynamics (Dufourc, 2008). Raft-like microdomains have a recognized regulatory role in mitochondria (Garofalo et al., 2015). These considerations draw attention to mitochondrial fatty acids and sterols as key lipid molecules involved in the structural arrangement of mitochondrial membranes.

Most studies on lipid-protein interactions have been carried out on mammalian mitochondria, due to the relevant implications in physiology and pathology (Di Donato, 2000). In recent years, the high nutritional and economic value of some cultivated bivalve mollusks elicited increasing interest in molluscan mitochondrial functions, since the capability to survive and grow implies good mitochondrial efficiency (Martinez et al., 2017),

In spite of the phylogenetic and biological distance, the Mediterranean mussel (*Mytilus galloprovincialis*) exhibits astonishing similarities to mammals in the mitochondrial F_1F_O-ATPase (E.C. 3.6.3.14) machinery (Nesci et al., 2013) as well as in the enzyme response to environmental pollutants (Pagliarani et al., 2013). On the other hand, even if the available information on the physico-chemical properties of molluscan mitochondrial membranes is still scanty, some peculiarities previously pointed out (Fiorini et al., 2016), which strongly differentiate mussel mitochondria from mammalian ones, open the door to intriguing interrogatives. Accordingly, if the basic features of mussel gill membrane lipids were somehow expected (Milkova et al., 1985; Fiorini et al., 2012), the maintenance of an unusual dis-homogeneous physical state of mitochondrial membranes, well compatible with the functioning of the F_1F_O-ATPase, the key enzyme in energy production, emerged as an amazing result (Fiorini et al., 2016). The Bivalvia class, widely represented in marine ecosystems, includes

89 highly diversified species which inhabit differently-featured habitats. In spite of their overall
90 similarity in shape, bivalve species cope with diversified environmental challenges.
91 Since 1983, when the Philippine clam *Ruditapes philippinarum* (Adams & Reeve, 1850), also
92 known as Manila clam, was first introduced in Italy, this alien species showed an increasing
93 success, up to gradually overwhelm the native clam species (*Ruditapes decussatus*) (Nerlovic
94 et al, 2016) and become a major economic resource for Italian shellfish culture (Sicuro et al.,
95 2016).
96 Based on these considerations, two questions promptly emerge. First: do different bivalve
97 species share the same basic features of mitochondrial membranes? In reality, the mitochondrial
98 envelope comprises two distinct membranes separated by the intermembrane space. However,
99 the inner membrane, which hosts the respiratory chain complexes and the F_1F_O-ATPase, gives
100 the main contribution to the composition of mitochondrial preparations, due to the extended
101 surface resulting from the *cristae* (Schenkel and Bakovic, 2016; Fiorini et al., 2016).
102 At present, we still wonder if the membrane physical state in mussel mitochondria (Fiorini et
103 al., 2016) should be considered as a species peculiarity or, alternatively it represents a widely
104 diffused membrane texture in mollusks. In the membrane arrangement, these organisms have
105 to exploit a lipid composition featured by abundant polyunsaturated fatty acids, mainly of the
106 *n*-3 series (Fiorini et al., 2012), and phytosterols, which in mussel mitochondria attain similar
107 levels to cholesterol (Milkova et al., 1985). A second, but not less attractive question can be
108 expressed as follows. On considering that mitochondrial membranes host the bioenergetic
109 machinery of the cell, may the membrane features contribute to the manifest resilience of
110 Manila clams to unfavourable environmental conditions (Kang et al., 2016; Nerlovic et al.,
111 2016) and, consequently, to its great adaptive success?
112 Keeping these objectives in mind, the present work combines biochemical and biophysical
113 approaches to explore the physico-chemical features of Manila clam gill mitochondrial
114 membranes and their relationship with the membrane-bound F_1F_O-ATPase activity, of key role

in cell bioenergetics. The comparison with mammalian and mussel mitochondrial membranes, which aims at pointing out peculiarities and similarities, may help to cast light on the link between the membrane physical state and the F_1F_O-ATPase efficiency. Fluorescence spectroscopy studies carried out in parallel on mitochondrial membranes and on liposomes obtained from total lipid extracts of mitochondria aim at clarifying the impact of lipid-protein interactions.

Preliminary data from these studies were presented as poster at the 67th National Conference of the Italian Physiological Society (Fiorini et al., 2016) and 48th National Conference of the Italian Marine Biology Society (Pagliarani et al, 2017).

2. Materials and methods

2.1. Animals

Adult clams (*Ruditapes philippinarum* Adams & Reeve, 1850), were obtained from coastal culture plants in transition waters (Sacca di Goro, near Po delta) in proximity of the Northern Adriatic Sea at the end of February. Water temperature was around 10°C (Arpae, 2017). Clams were transported alive in aerated seawater tanks to the laboratory. Approximately 250 healthy individuals of both sexes and of commercial size (≥25 mm shell length) were divided into pools of 50 animals each and used for the preparation of mitochondrial fractions.

2.2. Preparation of mitochondrial fractions

After dissection of clams, the gills were quickly removed from the soft tissue, pooled, repeatedly rinsed in ice-cold washing Tris–HCl buffer consisting of 0.25 M sucrose, 5 mM Tris(hydroxymethyl)-aminomethane (Tris), pH 7.4. Once rinsed, the tissues were gently dried on blotting paper, weighted and homogenized in the homogenizing buffer (0.25 M sucrose, 24 mM Tris, 1.0 mM EDTA, 0.5 mg/mL fatty acid-free bovine serum albumin (BSA), pH 7.4 with HCl, in the proportion 11 mL homogenizing buffer for each g (gill wetmass), by Ultraturrax

T25 (IKA-Labortechnik) at 14,000 rpm for 1 min. The mitochondrial fraction was obtained by stepwise centrifugation (Sorvall RC2-B, rotor SS34) from the homogenate. Gill homogenate was first centrifuged at 1500 *g* for 10 min; the obtained supernatant was filtered through four gauze layers and further centrifuged at 9000 *g* for 12 min to yield the raw mitochondrial pellet. Finally, the raw mitochondrial pellet was resuspended by gentle stirring using a Teflon Potter Elvejehm homogenizer in a small volume of homogenizing buffer and further centrifuged at 9000 *g* for 12 min to obtain the final mitochondrial pellet. The latter was gently resuspended in small aliquots of homogenizing buffer solution to attain a concentration of 15 – 20 mg/mL protein. Protein concentration was determined by Bio-Rad Protein Assay kit II with BSA as standard according to the colorimetric method of Bradford (1976). All centrifugation steps were carried out at 0–4 °C. The mitochondrial preparations were then stored in small aliquots (1-2 mL) in liquid nitrogen until use, a protocol already proven to preserve the mitochondrial F_1F_O–ATPase activity for years (Pagliarani et al., 2008a).

Prior to storage, the respiratory activities were polarographically evaluated (Chance and Williams, 1956) on freshly prepared mitochondrial membranes as previously described (Nesci et al, 2011), to check their functionality. These tests, combined with the failed detection of the Na,K-ATPase activity, a known marker of plasma membranes (Pagliarani et al., 2008b), witnessed the quality and the virtual absence of contamination of mitochondrial preparations (Nesci et al., 2012).

2.2. Lipid analyses

Lipid analyses were performed on gill mitochondrial preparations from 3-4 distinct animal pools. Since each pool consisted of 50 animals, replicates were considered adequate to take into account the biological variability among individuals. Total lipids were extracted from mitochondria with chloroform/methanol 2:1(v/v) containing 0.01% butylated hydroxytoluene as antioxidant, by Folch's method (Folch et al., 1957). Fatty acid methyl esters, obtained by

total lipid transmethylation (Morrison and Smith, 1964), were analyzed on a Varian 3380 gas–liquid chromatograph equipped with a fused silica capillary column DB-23 (J&W Scientific) (30 m, 0.25 mm) and a flame ionization detector at 300 °C. The carrier gas was nitrogen at a flow rate of 1.2 mL/min. The oven temperature was set in programmed mode from 150 to 230 °C at 5 °C/min and then held at 230 °C for 5 min. Data were processed using a Varian Star Chromatography Workstation. Fatty acid methyl ester mixtures were identified by a combination of different procedures including their retention times, equivalent chain length, and comparison with known standards (marine polyunsaturated fatty acids [PUFA] no. 1 and 37-component fatty acid methyl esters (FAME) mix, Supelco), and known PUFA mixtures (Ventrella et al., 2008). The location of double bonds in unsaturated fatty acids was assessed as in a previous work (Fiorini et al., 2016).

Sterol analyses were carried out as in a previous work (Fiorini et al., 2016). Total sterols were colorimetrically evaluated by the assay kit BioVision K603-100. To evaluate sterol composition, after extraction of the unsaponifiable matter from crude lipid extracts of mitochondria, desmethylsterols and 4α-methylsterols were separated from other non-sterol components by thin layer chromatography (TLC) and acetylated by an Ac_2O/pyridine mixture (Pistocchi et al., 2005). Sterols were then analyzed on a Fisons HRGC 5160 MEGA gas-chromatograph equipped with an OV1 capillary column (25 m × 0.32 mm) and a flame ionization detector at 305 °C. The carrier gas was hydrogen at a flow rate of 1.7 mL/min. The oven temperature was set in isotherm mode at 280 °C. Individual sterols were identified on the basis of their retention times and characteristic fragmentation patterns in mass spectra as detailed in a previous work (Fiorini et al., 2016). Chrom-Card (Fisons Instruments) was used for data handling.

2.3. Preparation of lipid vesicles (liposomes)

Mitochondrial total lipid extracts from three distinct animal pools were dried under nitrogen flow and resuspended in the same media employed for the isolation of mitochondria. Multilamellar liposomes were obtained by vortexing the lipid suspensions. The absence of peroxidized phospholipids was checked in all the samples by measuring the oxidation index (Konings, 1984).

2.4. Temperature dependence of the F_1F_O–ATPase activity

Immediately after thawing, the mitochondrial fractions were used for the F_1F_O–ATPase activity assays as previously described (Fiorini et al., 2016). The method is based on the colorimetric evaluation of the concentration of inorganic phosphate (Pi) hydrolyzed by known amounts of mitochondrial protein, which indirectly measures the ATPase activity (Fiske and Subbarow, 1925), namely the F_1F_O complex hydrolytic capability. The enzyme activity was assayed in triplicate in a reaction medium (1 mL) containing 0.15 mg mitochondrial protein, 75 mM ethanolamine–HCl buffer, pH 8.9, 2.0 mM $MgCl_2$ plus 5.0 mM Na_2ATP. After 5 min preincubation at selected temperatures in the range 12-37 °C, with 2-3° intervals, the reaction, carried out at the same temperature of the preincubation, was started by the addition of the ATP substrate and stopped after 5 min by 1 mL ice-cold 15% (w/w) aqueous solution trichloroacetic acid. Then, the Pi concentration was colorimetrically evaluated on 500 µL of the supernatant obtained from the centrifugation for 15 min at 5000 rpm (ALC 4225 Centrifuge). Preliminary experiments assessed the linearity of enzyme activity as a function of time under the assay conditions employed. The F_1F_O–ATPase activity was calculated from the difference between the Pi hydrolyzed in the absence and in the presence of 4 µg/mL oligomycin, known inhibitor of the mitochondrial ATPase activity (Nesci et al., 2013). The enzyme activities, calculated as µmoles Pi mg protein^{-1} min^{-1}, were expressed as the mean ± SE of four determinations carried out on different mitochondrial preparations. The temperature dependence of the F_1F_O-ATPase activity was investigated by building the Arrhenius plot. To this aim, the enzyme activity at

each assay temperature was taken as the expression of the reaction rate constant *k*. By plotting ln *k* (ordinate) against the reciprocal of the absolute assay temperature in Kelvin (1/T) (abscissa), according to the linear expression of the Arrhenius equation:

$$\ln k = \ln A - E_a/RT \quad (1)$$

in which A corresponds to the fraction of molecules that would react in the absence of activation energy barrier, two straight lines were obtained. The correlation coefficients never lower than 0.98, confirmed their linearity. The intersection between these two lines corresponds to the temperature of discontinuity (Td) (x-axis), usually related to sharp membrane phase changes (Kumamoto et al., 1971). The activation energy (E_a) was directly calculated from the slope (changed to positive) of each straight line, multiplied by the gas constant R. According to the units employed, the activation energies were expressed as Kcal/mole. Each set of experiments, carried out on a selected mitochondrial preparation yielded an Arrhenius plot. The obtained data (E_a and Tm) were averaged and given as mean data from three replicates from preparations from distinct animal pools. which, due to high number of clams forming each pool, were considered adequate to take into account the individual biological variability.

2.5. Fluorescence measurements

Thawed mitochondrial preparations and lipid vesicles, immediately after their preparation, were used for fluorescence measurements, by using the fluorescent probe Laurdan (6-Dodecanoyl-2-dimethylaminonaphthalene), able to detect changes in membrane phase properties (Harris et al., 2002). Laurdan locates at the hydrophobic-hydrophilic interface of the membrane (Antonellini et al.,1998) with no partition between gel and liquid-crystalline phases (Parasassi et al., 1991). Laurdan fluorescence excitation and emission spectra are sensitive to the polarity and to the water dipolar relaxation around its chromophore (Parasassi et al.,1994). Since the movements of water around the probe depend on lipid packing, its fluorescence spectra are sensitive to membrane fluidity and disorder in the microenvironment where it is embedded

(Parasassi et al.,1994), showing a maximum emission near 440 nm in pure phospholipid gel phase and a shift to 490 nm in liquid-crystalline phase (Parasassi et al, 1990). The excitation generalized polarization at 360 nm (Ex GP^{360}) quantitatively relates Laurdan emission spectral shift and it is sensitive to the extent of water dipolar relaxation process: a decrease of Ex GP^{360} value means an increase in dipolar relaxation, indicating a more fluid microenvironment. The parameter Ex GP^{360} was calculated by measuring the fluorescence intensity at the emission wavelengths of 430 nm and 490 nm (λ_{exc} = 360 nm) according to the following formula (Parasassi et al. 1991):

$$ExGP^{360} = I_{430} - I_{490} / I_{430} + I_{490} \quad (2)$$

Laurdan excitation and emission generalized polarization (ExGP and EmGP) spectra, which give information about the phospholipid phase of the membrane, were derived from Laurdan spectroscopic data by the following equations (Bagatolli et al.,1999):

$$ExGP = I_{430} - I_{490} / I_{430} + I_{490} \quad (3)$$

where I_{430} and I_{490} are the intensities at each excitation wavelength, from 320 to 420 nm, obtained using a fixed emission wavelength of 430 and 490 nm, respectively.

$$EmGP = I_{390} - I_{360} / I_{390} + I_{360} \quad (4)$$

where I_{390} and I_{360} are the intensities at each emission wavelength, from 420 to 550 nm, obtained using a fixed excitation of 390 and 360 nm, respectively.

Laurdan Ex and Em GP spectra are wavelength independent when the membrane is in a gel phase; in the liquid-crystalline (LC) phase, Ex GP values decrease with increasing excitation wavelength, and the Em GP values increase with increasing emission wavelength. With two coexisting phases, the GP spectrum has an opposite trend to that of the LC phase (Parasassi et al., 1993).

Laurdan steady-state fluorescence measurements at 10°, 20° and 30 °C were carried on with a computer-controlled PerkinElmer LS55 spectrofluorimeter. The temperature was measured in

265 the sample by a digital thermometer. Final lipid–probe molar ratio was 1000:1. The
266 fluorescence measured in the membranes without Laurdan was always subtracted from the data.
267 Each Laurdan spectrum is the mean of three different determinations performed on distinct
268 animal pools.

269 *2.6. Calculations and statistics*

270 Statistical analyses on fatty acid and sterol composition, as well as on Arrhenius plot data were
271 performed by SIGMASTAT software. The analysis of variance followed by Students–
272 Newman–Keuls' test when F values indicated significance ($P \leq 0.05$) was applied. Percentage
273 data were arc*sin*-transformed before statistical analyses to ensure normality. Laurdan excitation
274 and emission spectra were normalized by using PerkinElmer FLWinLab Software. The
275 statistical significance of $ExGP^{360}$ values was evaluated by Student's t-test ($P \leq 0.05$).

276 # 3. Results

277 ## *3.1. Fatty acid and sterol composition of clam gill mitochondria*

278 The fatty acid composition of mitochondria is usually taken as a chemical clue of the membrane
279 physical state, being fatty acid unsaturation traditionally associated with membrane fluidity
280 (Logue et al., 2000). In isolated mitochondria the fatty acid composition largely mirrors that of
281 the inner mitochondrial membrane which hosts the F_1F_O-ATPase, due to the large extension of
282 invaginations forming the *cristae* (Schenkel and Bakovic, 2014), in turn accounting for most of
283 the inner membrane surface (Kuhlbrandt, 2015).

284 Manila clam gill mitochondria exhibit the typical marine fatty acid pattern (Table 1).
285 Accordingly, polyunsaturated fatty acids (PUFA) attain 70.3 % of total fatty acids. Among
286 PUFA, *n*-3 fatty acids largely prevail on *n*-6 fatty acids (44.9 *vs* 9.7 %), with a prominent
287 contribution of docohexaenoic acid (DHA). Interestingly, non-methylene interrupted fatty acids

(NMI), featured by an unusual unsaturation pattern, namely more than two single bonds between two subsequent double bonds, typical of marine invertebrates (Barnathan, 2009) and especially abundant in membrane phospholipids (Ventrella et al., 2013) are approximately 15% of total fatty acids and mainly consist of C_{20} and C_{22} dienoic fatty acids. Consistently, the most abundant representatives 22:2 Δ 7,13 and 22:2 Δ 7,15 are the most often encountered NMI structures in mollusks (Barnathan, 2009). This fatty acid pattern, and especially the high DHA level, imply a high unsaturation index, which quantifies the high unsaturation of clam gill mitochondrial membranes.

Mitochondrial sterols have been neglected and even underestimated for long time, even if cholesterol and related compounds are long known as plastic components in membranes. However, recent advances point out that the level and molecular composition of sterols is crucial in the maintenance of the membrane physical state (Ollila et al., 2007; Dufourc, 2008) and may mirror evolutionary adaptations (Galea and Brown, 2009). Additionally, mitochondrial sterols now emerge as crucial membrane components and quali-quantitative changes in sterols are involved in physiology (Shi et al., 2013) and pathology (Fernandez et al., 2009; Bosch et al., 2011). Interestingly, in Manila clam gill mitochondria the total sterols reach 42 mg/g protein, a level twice as much as in mussel mitochondria (Fiorini et al., 2016), confirming that bivalve molluscan sterols in mitochondria are much more abundant than in mammals (5 mg/g protein in swine heart mitochondria) (Fiorini et al. 2016), Additionally, the sterol pattern in mitochondria reveals some interesting features. All the identified sterols are Δ^5 sterols. As shown in Table 2, where both clam and mussel gill mitochondrial sterols are presented to facilitate the comparison between the two species, cholesterol, the main zoosterol, only represents 42%, consistently with previous reports in bivalve mollusks (Milkova et al., 1985; Fiorini et al., 2016). Phytosterols, structurally related to cholesterol, but differing from cholesterol in the unsaturated and differently branched hydrocarbon side chain, and most likely

313 of algal origin in bivalve mitochondria, roughly constitute the remaining half of total sterols. In
314 comparison with mussel mitochondria, clam gill mitochondria exhibit a wider phytosterol
315 pattern, which also embraces fucosterol (less than 1%) and the three major phytosterols in
316 nature (Lizard, 2011), namely stigmasterol, β-sitosterol and campesterol, which taken together
317 approximately amount to 10% of total sterols. Other phytosterols, such as brassicasterol, 24-
318 methylene cholesterol and 22-dehydrocholesterol, attain similar percentages to mussel gill
319 mitochondrial ones (Fiorini et al., 2016). The percentage of desmosterol, known as unsaturated
320 cholesterol precursor in mammals (Huster et al., 2005), is halved in clams with respect to mussel
321 gill mitochondria.

322 *3.2. Activation energies of the F_1F_O-ATPase activity*

323 The activation energy of an enzyme reaction, calculated from the Arrhenius plot, constitutes
324 the energy barrier that must be overcome to yield the product. In other words, low activation
325 energies are usually associated with efficient enzyme catalysis. As for other membrane-bound
326 enzymes, the Arrhenius plot of the mitochondrial F_1F_O-ATPase is currently reported as
327 discontinuous (Solaini and Bertoli, 1981; Fiorini et al., 2016), namely it consists of two straight
328 lines with different slopes. Consistently, two distinct activation energies exist, obtained from
329 the slopes above and below the so-called temperature of discontinuity (Td), which is currently
330 taken as correspondent to an abrupt change in membrane physical state. When the activation
331 energies of clam gill mitochondrial F_1F_O-ATPase activity are compared with that obtained in
332 mussel gill and mammalian mitochondria (Fiorini et al., 2016) (Table 3), they are significantly
333 lower both above (Ea_1) and below (Ea_2) the Td, which, in spite of minor fluctuations, lies in the
334 20-22°C range in all the three species mitochondria.

335 3.3.*Fluorescence measurements*

To detect changes referable to lipid-protein interactions, fluorescence measurements were carried out in parallel on gill mitochondrial membranes and on liposomes prepared with total lipid extracts from gill mitochondria. Laurdan normalized excitation and emission spectra in clam gill mitochondria at 10°, 20° and 30°C are shown in Fig. 1. The excitation spectrum shows two peaks: the former at ~ 357nm and the latter at ~ 390 nm. At all the temperatures tested, the 390/360 ratio is <1 and the peak at 390 nm decreases by increasing the temperature. The emission spectrum has a peak at ~ 437 nm at all temperatures, and an increase of intensity in the red band of the spectrum as the assay temperature increases, due to the solvent relaxation. Fig. 2 shows Laurdan normalized excitation and emission spectra in liposomes prepared with clam gill mitochondrial lipids. The excitation spectrum shows two peaks: at 10°C and 20°C the former is at ~ 357 nm and the latter at ~ 390 nm; at 30°C the former and highest peak has a shift at 354 nm. The 390/360 ratio is <1 at the three temperatures tested and the peak intensity at 390 nm decreases by increasing the assay temperature. The emission spectrum shows a maximum at ~ 434 nm at 10°C and 20°C and at 432 nm at 30°C and an increase in the red band intensity of the spectrum as the assay temperature increases.

Table 4 shows the Laurdan Ex GP^{360} values at 10, 20, 30 °C, calculated according to the equation (2) in Section 2.5 in mitochondrial membranes of clam and mussel gills and of swine heart and in liposomes prepared from total lipid extracts of mitochondria of these tissues. For comparative purpose, calculated data from previously obtained spectra (Fiorini et al., 2016) are listed below those obtained in the present work. In all samples the $ExGP^{360}$ values are quite high at all temperatures; in clam and swine mitochondrial membranes and in liposomes of the three tissues the Ex GP^{360} values show a significant gradual decrease by increasing the assay temperature. On the other hand, in mussel gill mitochondrial membranes the Ex GP^{360} values are not affected by the assay temperature, and only in liposomes a significant decrease at 30°C is shown, even if the Ex GP^{360} value is much higher than that in mitochondrial membranes.

Laurdan excitation and emission GP spectra in clam gill mitochondria are shown in Fig. 3. Both excitation (Fig. 3A) and emission (Fig. 3 B) GP spectra show a pattern typical of the LC state, even though the values are relatively high. While the excitation GP spectra are affected by temperature, showing a decrease in the values at increasing temperatures, the GP emission values are very little affected by the assay temperature.

Fig. 4 shows Laurdan excitation and emission GP spectra in liposomes prepared with lipids extracted from clam gill mitochondria. The excitation (Fig. 4A) and emission (Fig. 4B) GP spectra show the typical pattern of LC state with relatively high values. All the GP spectra of liposomes are affected by temperature as the values decrease at increasing temperatures. The emission GP values in liposomes are significantly higher than those in mitochondrial membranes at all the temperatures tested.

4. Discussion

4.1. Lipid features and clues on the membrane arrangement

Manila clam gill mitochondrial lipids exhibit peculiar features, among which the high content of sterols with a widely diversified sterol pattern appears as the most interesting property. Accordingly, the highly unsaturated fatty acid composition in Manila clam gill mitochondria is not substantially different from that detected in mussel gill mitochondria. The high mitochondrial DHA content is consistent with the fatty acid selectivity of cardiolipin, an unique dimeric phospholipid which attains up to 20% of total phospholipids in the inner mitochondrial membrane (Mejia and Hatch, 2016), rules respiratory complexes and the ATP synthase (Mejia and Hatch, 2015; Mehdipour and Hummer, 2016) and in this species contains at least two DHA molecules (Kraffe et al., 2005). The mitochondrial membrane fatty acid composition in mollusks is known to be affected by the lipid dietary input, the physiological status of the species and environmental conditions, especially temperature (Gillis and Ballantyne, 1999). So, the mitochondrial membrane is continuously remodeled, and, even if clams and mussels were

386 sampled in the same period, they came from different habitats. However, gill structural lipids
387 have a species-specific composition (Delaporte et al., 2005), being less susceptive to changes
388 than other tissue mitochondria. Moreover, structural lipids from different organs of *R.*
389 *philippinarum*, a species which differs from other mollusks in structural and functional
390 properties of mitochondrial membranes, have a different fatty acid composition (Kraffe et al.,
391 2015). Most likely, this tissue-specific composition occurs in all molluscan species. These
392 considerations corroborate the choice of gill mitochondria to allow comparison between mussel
393 and Manila clam.
394 Among unsaturated fatty acids, NMI fatty acids (Fiorini et al., 2016), whose peculiar
395 unsaturation pattern makes the molecule less flexible with respect to commonly unsaturated
396 fatty acids (Rabinovich and Ripatti, 1991) and, as far as we are aware, lack in mammalian
397 membranes (Barnathan, 2009), approximately attain the same percentage on total fatty acids in
398 clam and mussel mitochondria (Fiorini et al., 2016). However, on considering the membrane
399 arrangement, it seems worthwhile noticing that, while saturated fatty acids tend to exclude
400 cholesterol, due to their straight shape and tight packing, unsaturated fatty acids are well
401 compatible with the bulky sterol insertion (Shimokawa et al., 2017). So, a physical link exists
402 between unsaturated fatty acid and sterol content, since highly unsaturated acyl chains seem to
403 favor sterol incorporation. Interestingly, the relatively high sterol level in clam mitochondria
404 not only may *per se* affect the membrane physical state, but also have a protective task.
405 Accordingly, even if currently considered minor lipid components of mitochondrial
406 membranes, (Valencak and Azzu, 2014), mitochondrial sterols attain increasing interest, being
407 involved not only in mitochondrial dysfunctions (Bosch et al., 2011), but also in the protection
408 against the oxidative stress (Galea and Brown, 2009). The high unsaturation makes molluscan
409 mitochondrial membrane lipids especially prone to peroxidation. Mitochondrially-generated
410 reactive oxygen species attack methylene bridges adjacent to unsaturated carbon bonds in fatty
411 acids (Valencak and Azzu, 2014). So, the co-occurrence of NMI fatty acids, which inhibit

412 peroxidation (Zakhartsev et al., 1998), and of relatively abundant sterols may represent
413 complementary strategies to counteract oxidative stress in the highly unsaturated molluscan
414 mitochondrial membranes. While the basic molecular arrangement of mitochondrial
415 membranes is apparently not substantially different between mussels and clams, the physical
416 state is clearly affected by the specific sterol composition. At least some of the effects ascribed
417 to mitochondrial sterols may rely on their plasticity. Accordingly, membrane phytosterols are
418 not only involved in the homeoviscous adaptation of marine organisms (Pernet et al., 2009),
419 but also extend the temperature range in which the membrane-associated processes can take
420 place (Dufourc, 2008). Assumed that sterols modulate membrane properties (Falcioni, 2012),
421 different sterols may have different modulatory roles. The complex mixture of C_{26} to C_{29} sterols
422 in clam gill mitochondria is somehow simplified in mussel gill mitochondria which apparently
423 lack C_{29} sterols (Fiorini et al., 2016). All these molecular species share a planar ring system
424 with a 3β hydroxyl group, while the side chain has a varying length. An increase or decrease in
425 one or more carbons is known to affect membrane order (Dufourc, 2008), especially by
426 modifying the tilt of the sterol ring system, which in turn depends on all interactions between
427 the sterols and the other membrane components. Even if computer simulation results should be
428 taken with caution, cholesterol and desmosterol, the latter differing from cholesterol only by
429 one double bond in the hydrocarbon tail, were reported to produce almost identical effects on
430 unsaturated bilayers (Rȍg et al., 2009). However, if the hydrocarbon chain complexity
431 increases, things may be different. Generally, an increase in tail length not only increases
432 hydrophobicity (Dufourc, 2008), but also affects the spatial arrangement of the molecule since
433 the moiety with tetrahedral arrangement of carbon atoms increases. Therefore, branched-chain
434 sterols are likely to produce different effects from cholesterol. Accordingly, the branched-chain
435 C_{29} sterols, even if less than 10% of all sterols, may significantly contribute to the peculiar
436 membrane environment in clam gill mitochondria, affecting the membrane organization, as
437 shown both by Laurdan GP spectra and by Laurdan emission and excitation spectra. In

mitochondrial membranes and in liposomes prepared with clam gill mitochondrial lipids the excitation and emission GP spectra show the typical profile of a LC phase, while the relatively high values, even at 30°C, of the excitation spectra are typical of cholesterol-rich membranes (Parasassi et al, 1994). Quite surprisingly, this pattern, very different from that detected in liposomes obtained from mussel gill mitochondrial lipids, is similar to that found in liposomes from mammalian mitochondrial lipids (Fiorini et al. 2016).

To sum up, in spite of the known mitochondrial plasticity, it seems reasonable to assume that the basic structural arrangement of clam gill mitochondrial membranes, which leads to a peculiar physical state, is representative of the molecular strategy of the species.

4.2. Response to temperature changes

One of the goals of this work was to explore how gill mitochondrial membranes respond to temperature changes, on considering both the membrane physical state and the F_1F_O-ATPase activity. Some clues came from fluorescence spectroscopy data. Accordingly, while in clam mitochondrial membranes at the three temperatures tested the Laurdan emission spectra with a maximum at 437 nm seem to reproduce the gel phase spectra in artificial membranes, the excitation spectra with a 390/360 ratio <1 are indicative of a LC phase. This puzzling coexistence was also reported in synthetic phospholipid and cholesterol liposomes (Parasassi et al, 1992). Since in liposomes obtained from clam gill mitochondrial lipids both the emission and excitation maxima at 30°C shifted with respect to those at 10° and 20°C (which show identical wavelength), namely 432 nm vs437 nm and 354 nm vs 357 nm, respectively, we can speculate that the high level of n-3 PUFA-containing phospholipids can modulate the interactions between fatty acid acyl chains, and particularly between fatty acyl chains and sterols, to produce a peculiar membrane texture. Consistently, n-3 PUFA were recently reported to modify membrane organization in model systems (Wassall et al., 2009; Shaikh et al., 2015)

462 and in some cell types (Turk et al., 2013; Shaikh et al., 2015), thus affecting cellular functions,
463 as reported by Hou et al., 2016 in $CD4^+$ T cells.
464 The Ex GP^{360} values in mitochondrial membranes and liposomes of both clam gills and swine
465 heart (Table 4), in spite of their different fatty acid composition (Fiorini et al., 2016), are
466 temperature-sensitive. In simple terms, if temperature increases from 10 to 30°C the
467 mitochondrial membrane environment in Manila clams exhibits the same behavior as in
468 mammals. Most likely, the relatively abundant sterols in clam mitochondrial membranes may
469 modulate the molecular interactions among membrane components, so as to facilitate
470 membrane-bound enzyme catalysis, as the quite low F_1F_O-ATPase activation energies above
471 and below the break strongly suggest (Table 3). In model systems C_{29} phytoterols such as
472 stigmasterol and sitosterol are known to decrease membrane order in comparison with
473 cholesterol (C_{27}). The branched ethyl groups would increase membrane cohesion through the
474 formation of smaller membrane domains, thus playing a crucial role in membrane dynamics
475 and function (Dufourc, 2008). Interestingly, in mussel gill mitochondrial membranes, which,
476 on the basis of our findings, mainly differ from clam gill mitochondrial membranes in the lack
477 of C_{29} sterols and campesterol, the Ex GP^{360} values are temperature-insensitive (Table 4), and
478 the F_1F_O-ATPase activation energies approach the swine heart mitochondrial ones (Table 3).
479 These intriguing clues suggest that branched-chain sterols, even if in low amounts, may be
480 crucial in modulating the membrane physical state. The differences between mitochondrial
481 membranes and liposomes stress the relevance of lipid-protein interactions.
482 To sum up, we can hypothesize that, due to the peculiar molecular interactions in clam
483 mitochondrial membranes in which structural lipid components, namely phospholipids
484 containing PUFA and NMI fatty acids, phytosterols and cholesterol, coexist with membrane-
485 bound proteins, the membrane microenvironment of the F_1F_O–ATPase may somehow favor the
486 enzyme activity so as to facilitate catalysis in a wide temperature range. This means that also at
487 temperatures above 22°C (break in the Arrhenius plot), and consistently with the species

thermal resistance (Velez et al., 2017), the mitochondrial membrane is maintained in a physical state well compatible with the F_1F_O-ATPase function.

5. Conclusion

The present work points out how, based on the different molecules available for the mitochondrial membrane constitution, bivalve mollusks seem to adopt different molecular strategies. The findings can be taken as a sort of picture of the membrane state, which, focused on crucial membrane components and irrespective of remodeling, provides clues on the molecular strategy of the species. Undoubtedly, lipid-protein interactions, but also lipid-lipid interactions, play a key role in the maintenance of mitochondrial membranes in a peculiar physical state. Most likely, mussels and clams have different threads available to make their mitochondrial membrane texture and assemble them in a different way. In clam mitochondria the maintenance of a quite homogeneous enzyme microenvironment favors the F_1F_O-ATPase functionality, by lowering the enzyme activation energies, in a wide temperature range.

The molecular assembly which produces the peculiar physical features of clam mitochondrial membranes may be one among the biochemical properties which contribute to limit the oxidative damage, maintain the mitochondrial efficiency and mitigate the effects of temperature increase (Velez et al., 2017), thus favoring the great adaptive success of *R. philippinarum* in the Adriatic Sea shallow waters, featured by wide temperature oscillations (Russo et al., 2012; Arpae, 2017).

6. Funding

This work was financed by a RFO grant from the University of Bologna and by a RSA grant from the Marche Polytechnic University.

7. Competing interest

All authors declare no conflict of interest.

513

514 8. List of symbols and abbreviations

515 BSA, bovine serum albumin; DHA, docohexaenoic acid; Ex GP^{360}, excitation generalized
516 polarization at 360 nm; GP, generalized polarization; *Ea,* activation energy EDTA, ethylene
517 diamminotetraacetic acid; Laurdan, 6-Dodecanoyl-2-dimethylaminonaphthalene; LC, liquid
518 crystalline; NMI, non-methylene interrupted; PUFA, polyunsaturated fatty acids; TLC, thin
519 layer chromatography; Tm, melting temperature; Tris, Tris(hydroxymethyl)-aminomethane.

520 9. References
521

522 Antollini, S.S., Barrantes, F.J. 1998. Disclosure of discrete sites for phospholipids and sterols
523 at the protein-lipid interface in native acetylcholine receptor-rich membrane. *Biochemistry* 37,
524 16653-16662.

525 Arpae 2017. Monitoraggio delle acque di transizione e classificazione dello stato di qualità.
526 Regione Emilia-Romagna. Rapporto triennale 2014-2016.
527 https://www.arpae.it/cms3/documenti/daphne/download/rapporto_2014-2016_transizione.pdf

528 Bagatolli, L.A., Parasassi, T., Fidelio, G.D., Gratton, E. 1999. A model for the interaction of 6-
529 Lauroyl-2-(N,N-dimethylamino)naphthalene with lipid environments: implications for spectral
530 properties. *Photochem. Photobiol*. 70, 557-564.

531 Barnathan, G. 2008. Non-methylene interrupted fatty acids from marine invertebrates.
532 Occurrence, characterization and biological properties. *Biochimie* 91, 671-678.

533 Bradford, M.M. 1976. A rapid and sensitive method for quantification of microgramquantities
534 of protein utilizing the principle of protein-dye binding. *Anal. Biochem*. 72, 248–254.

535 Bosch, M., Monserrat M., Gross, S.P., Fernandez-Checa, J.C., Pol, A. 2011. Mitochondrial
536 cholesterol: a connection between caveolin, metabolism and disease. *Traffic* 12, 1483-1489.

537 Chance, B., Williams, G.R. 1956. The respiratory chain and oxidative phosphorylation. *Adv.*
538 *Enzymol*. 17, 65–134.

539 Delaporte, M., Soudant, P., Moal, J., Kraffe E., Marty, Y.. Samain, J.F. 2005. Incorporation and
540 modification of dietary fatty acids in gill polar lipids by two bivalve species, *Crassostrea gigas*
541 and *Ruditapes philippinarum*. *Comp. Biochem. Physiol A* 140, 460-470.

542 Di Donato, **S**. 2000. Disorders related to mitochondrial membranes: pathology of the respiratory
543 chain and neurodegeneration. J. Inherit. *Met. Dis.* 23, 247-63.

544 Dufourc, E.J. 2008. Sterols and membrane dynamics. *J. Chem. Biol.* 1, 63-67.

545 Ernst, R., Ejsing, C.S., Antonny, B. 2016. Homeoviscous adaptation and the regulation of
546 membrane lipids. *J. Mol. Biol*. 428, 4776-4791.

547 Falcioni G. 2012. Biomembrane perturbation induced by organotins in model and biological
548 membranes. In: *Biochemical and biological effects of organotins*, (A. Pagliarani, F. Trombetti,
549 V. Ventrella eds.) Bentham Science Publishers, Ltd, pp. 70-74.

550 Fernandez, A., Llacuna, L., Fernandez-Checa J.C., Colell A. 2009. Mitochondrial cholesterol
551 loading exacerbates amyloid beta peptide-induced inflammation and neurotoxicity. *J. Neurosci*.
552 20, 6394-6405.

553 Fiorini, R., Pagliarani, A., Nesci, S., Pirini, M., Tucci, E. and Ventrella, V. 2012. Structural and
554 functional changes in gill mitochondrial membranes from the Mediterranean mussel *Mytilus*
555 *galloprovincialis* exposed tri-n-butyltin. *Environ. Toxicol. Chem*. 31, 877–884.

556 Fiorini, R. Nesci S., Ventrella V., Trombetti F., Fabbri M., Pagliarani A. 2016. Lipid
557 composition and physico-chemical properties of gill mitochondrial membranes from *Ruditapes*
558 *philippinarum.* 67th National Congress of the Italian Physiological Society, Catania, Italy 21-
559 23 September 2016, *Abstract book,*179.

560 Fiorini R., Pagliarani, A., Nesci, S., Trombetti, F., Pirini, M., Fabbri M. and Ventrella, V. 2016.
561 Lipid unsaturation *per se* does not explain the physical state of mitochondrial membranes in
562 *Mytilus galloprovincialis*". Comp. Biochem. Physiol. B 191: 67-75.

563 Fiske, C.G., Subbarow, Y. 1925. The colorimetric determination of phosphorus. *J. Biol.Chem*.
564 66, 375–400.

565 Folch, J., Lees, M., Sloane-Stanley, G.H. 1957. A simple method for isolation and purification
566 of total lipids from animal tissue. *J. Biol. Chem.* **226**, 497–509.

567 Galea, A.M. and Brown, A.J. 2009. Special relationship between sterols and oxygen: were
568 sterols an adaptation to aerobic life? *Free Rad. Biol Med.* **47**, 880-889.

569 Garofalo T., Manganelli, V., Grosso, M.; Mattei V., Ferry A., Misasi, S., Sorice, M. 2015. Role
570 of mitochondrial raft-like microdomains in the regulation of cell apoptosis. *Apoptosis* 20, 621-
571 634.

572 Gillis, T.E., Ballantyne, T.S. 1999. Influence of subzero thermal acclimation of mitochondrial
573 membrane composition of temperate zone marine bivalve mollusks. Lipids **34**, 59-66.

574 Harris, F.M., Best, K.B. Bell, J.D. 2002. Use of Laurdan fluorescence intensity and polarization
575 to distinguish between changes in membrane fluidity and phospholipid order. *Bioch. Biophys.*
576 *Acta Biomembranes* 1565, 123-128.

577 Hou, T.Y., McMurray, D.N., Chapkin, R.S. 2016. Omega-3 fatty acids, lipid rafts and T cell
578 signaling. *Eur. J. Pharm.*785, 2-9.

579 Huster, D., Scheidt, H.A., Arnold, K., Herrmann, A., Muller, P. (2005). Desmosterol may
580 replace cholesterol in lipid membranes. *Biophys. J*. 88, 1838-1844.

581 Kang, H.Y., Lee, Y.J, Choi, K.S, Park, H.J, Yun, S.G., Kang, C.K. (2016). Combined effects
582 of temperature and seston concentration on the physiological energetics of the Manila clam
583 *Ruditapes philippinarum* . *PLoS ONE* 11(3)e0152427. doi:10.1371/journal.pone.0152427

584 Konings, A.W.T. 1984. Lipid peroxidation in liposomes. In:, *Liposome Technology*
585 *Preparation of liposomes I.* (ed. G. Gregoriadis) pp. 139–161 CRC Press, Inc., Boca Raton,
586 Florida,

587 Kraffe E., Soudant P., Marty Y. and Kervarec, N. 2005. Docohexaenoic acid and
588 eicosapentaenoic acid-enriched cardiolipin in the Manila clam *Ruditapes philippinarum*. Lipids
589 40, 619-625.

590 Kuhlbrandt, W. 2015. Structure and function of mitochondrial membrane protein complexes.
591 *BMC Bio*. 13, 89. DOI 10.1186/s12915-015-0201-x

592 Kumamoto, J., Raison, L.K. and Lyons, J.M., 1971. Temperature "breaks" in Arrhenius plots:
593 a thermodynamic consequence of a phase change. *J. Theor. Biol.* **31**, 47–51.

594 Lizard, G. 2011. Impact of phytosterols on mitochondrial functions. *Br.J.Nutr.* **106**, 461-462.

595 Logue, J.A., De Vries, A.L., Fodor, E., Cossins, A.R. 2000. Lipid compositional correlates of
596 temperature-adaptive interspecific differences in membrane physical structure. *J. Exp, Biol.*
597 **203**, 2105-2115.

598 Los, D.A. and Murata, N. 2004. Membrane fluidity and its roles in the perception of
599 environmental signals. *Biochim. Biophys. Acta Biomembranes* 2666, 142-157.

600 Martinez, E., Menze, M.A. and Agosta, S.A. 2017. Reduced mitochondrial efficiency explain
601 mismatched growth and metabolic rate at supraoptimal temperatures. *Physiol. Biol. Chem.*
602 *Zool*. 90, 294-298.

603 Mejia, E.M. and Hatch, G.M. 2016. Mitochondrial phospholipids: role in mitochondrial
604 function. *J. Bioenerg. Biomembr.* 48, 99-112.

605 Mehdypour, A.R. and Hummer, G. 2016. Cardiolipin puts the seal on ATP synthase. *Proc. Natl.*
606 *Acad. Sci.* U.S.A. 113, 8568-8570.

607 Milkova, Ts, Stoilov, I., Popov, S., Charakchieva, S., Andreev, S. 1985. Subcellular distribution
608 of sterols in the mussel *Mytilus galloprovincialis*. *Comp. Biochem. Physiol. B* 81, 491–492.

609 Morrison,W.R., Smith, L.M. 1964. Preparation of fatty acid methylesters and dimethylacetals
610 from lipids with boron fluoride-methanol. *J. Lipid Res*. **5**, 600–608.

611 Nerlovic, V., Korlevic, M., Mravinak, B. 2016. Morphological and molecular differences
612 between the invasive bivalve *Ruditapes philippinarum* (Adams & Reeve, 1850) and the native
613 species *Ruditapes decussatus* (Linnaeus, 1858) from the Northeastern Adriatic Sea. *J. Shellfish*
614 *Res.* 35, 1-9.

615 Nesci, S., Ventrella, V., Trombetti, F., Pirini, M., Pagliarani, A. 2011. Tributyltin (TBT) and
616 mitochondrial respiration in mussel digestive gland. Toxicol. in Vitro 25, 951–959.

617 Nesci, S., Ventrella, V., Trombetti, F., Pirini, M. and Pagliarani, A**.** 2012. Tri-n-butyltin binding
618 to a low-affinity site decreases the F_1F_O–ATPase sensitivity to oligomycin in mussel
619 mitochondria. *Appl. Organomet. Chem.* 26, 593–599.

620 Nesci, S., Ventrella, V., Trombetti, F., Pirini, M., Pagliarani, A. 2013. Mussel and mammalian
621 ATP synthase share the same bioenergetic cost of ATP. *J. Bioenerg. Biomembr.* 45**,** 289–300.

622 Ollila, O.H.B., Rog, T., Karttunen, M. and Vattulainen, I. 2007. Role of sterol type on lateral
623 pressure profiles of lipid membranes affecting membrane protein functionality: comparison
624 between cholesterol, desmosterol, 7-dehydrocholesterol and ketosterol. *J. Struct. Biol* 159, 311-
625 323.

626 Pagliarani, A., Bandiera, P., Ventrella, V., Trombetti, F., Pirini, M., Nesci, S., Borgatti, A.R.,
627 2008a. Tributyltin (TBT) inhibition of oligomycin sensitive Mg–ATPase activity in mussel
628 mitochondria. *Toxicol. in Vitro* 22, 827–836.

629 Pagliarani A., Bandiera P., Ventrella V., Trombetti F., Manuzzi M.P., Pirini M. and Borgatti
630 A.R. 2008b. Response of Na^+-dependent ATPase activities to the contaminant ammonia
631 nitrogen in *Tapes philippinarum*: possible ATPase involvement in ammonium transport. *Arch.*
632 *Env. Contam. Toxicol.* 55, 49-56.

633 Pagliarani, A., Nesci, S. and Ventrella, V. 2013. Toxicity of organotin compounds: shared and
634 unshared biochemical targets and mechanisms in animal cells. *Toxicol. in Vitro* 27, 978–990.

635 Pagliarani, A., Fiorini, R., Nesci, S., Trombetti, F., Fabbri, M. and Ventrella V. 2017. Le
636 caratteristiche delle membrane mitocondriali della vongola *Ruditapes philippinarum* (Adams
637 & Reeve, 1850) possono contribuire al suo successo? *Biol. Mar. Medit. Proc. 48th National*
638 *Conf. It. Soc. Marine Biology* 24, 80-81

639 Parasassi, T., De Stasio, G., D'Ubaldo, A., Gratton, E. 1990. Phase fluctuation in phospholipid
640 membranes revealed by Laurdan fluorescence. *Biophys. J.* 57, 1179-1186.

641 Parasassi, T., De Stasio, G., Ravagnan, G., Rush, R.M., Gratton, E. 1991. Quantitation of lipid
642 phases in phospholipid vescicles by the generalized polarization of Laurdan fluorescence.
643 *Biophys. J.* 60, 179-189.

644 Parasassi, T., Di Stefano M., Ravagnan, G., Sapora, O., Gratton, E. 1992. Membrane aging
645 during cell growth ascertained by Laurdan Generalized Polarization. Exp. Cell Res. 202, 432-
646 439.

647 Parasassi, T., Loiero, M., Raimondi, M., Ravagnan, G., Gratton, E. 1993. Absence of lipid gel-
648 phase domains in seven mammalian cell lines and in four primary cell types. *Biochim. Biophys.*
649 *Acta* 1153, 143-154.

650 Parasassi, T., Di Stefano, M., Loiero, M., Ravagnan, G., Gratton, E. 1994, Influence of
651 cholesterol on phospholipid bilayers phase domains as detected by Laurdan fluorescence.
652 *Biophys. J*. 66, 120-132.

653 Pernet, F., Réjean, T., Gionet, C., Landry, T. 2009. Lipid remodeling in wild and selectively
654 bred hard clams at low temperatures. *J. Exp. Biol.* 209, 4663-4675.

655 Pistocchi, R., Trigari, G., Serrazanetti, G.P., Taddei, P., Monti, G., Palamidesi, S., Guerrini, F.,
656 Bottura, G., Serratore, P., Fabbri, M., Pirini, M., Ventrella, V., Pagliarani, A., Boni, L., Borgatti,
657 A.R., (2005). Chemical and biochemical parameters of cultured diatoms and bacteria from the
658 Adriatic Sea as possible biomarkers of mucilage production. *Sci.Total Environ.* 353, 287–299.

659 Rabinovich, A.L., Ripatti, P.O. 1991. The flexibility of natural hydrocarbon chains with non-
660 methylene interrupted double bonds. *Chem. Phys. Lipids* 58, 185-192.

661 Ròg, T., Pazenkiewicz-Gierula, M., Vattulainen, I., Karttunen, M. 2009. Ordering effects of
662 cholesterol and its analogues. *Biochim. Biophys. Acta* 1788, 97-121.

663 Russo, A. Carniel, S., Sclavo, M., Krzelj, M. (2012). Climatology of the Northern-Central
664 Adriatic Sea, In *Modern Climatology* (ed. S.Y. Wang), ISBN: 978-953-51-0095-9, InTech,
665 http://www.intechopen.com/books/modern-climatology/climatology-of-the-northern-central-
666 adriatic-sea

667 Saliba, A.E., Vonkova, I., Gavin, A.C. 2015. The systematic analysis of protein-lipid
668 interactions comes of age. Nat. Rev. *Mol. Cell. Biol.*16, 753-61.

669 Schenkel, L.C. and Bakovic, M. 2014. Formation and regulation of mitochondrial membranes.
670 *Int. J. Cell Biol.* 709828. http://dx.doi.org/10.1155/2014/709828 (13 pp.).

671 Shaikh, S.R., Kinnun, J.J., Leng, X., Williams, J.A., Wassal, S.R. 2015. How polyunsaturated
672 fatty acids modify molecular organization in membranes: insight NMR studies of model
673 systems. *Biochim. Biophys. Acta* 1848, 211–219.

674 Shi, C., Wu, F., Xu, J. 2013. Incorporation of β-sitosterol into mitochondrial membranes
675 enhances mitochondrial function by promoting inner membrane fluidity. *J. Bioen. Biomembr.*
676 45, 301-305.

677 Shimokawa, N., Mukai, R., Nagata, M., Tagagi. M. 2017. Formation of modulated phases and
678 domain rigidification in fatty acid-containing lipid membranes. *Phys Chem. Chem. Phys* 19,
679 13252-13263.

680 Solaini, G., Bertoli, E. 1981. Lipid dynamics and lipid-protein interactions in isolated beef-
681 heart mitochondrial ATPase complex. *FEBS Lett. 132,* 127-128.

682 Turk, H.F., Chapkin, R.S. 2013. Membrane lipid raft organization is uniquely modified by n-3
683 polyunaturated fatty acid. *Prostaglandin Leukot. Essent. Fatty Acids* 88, 43-47.

684 Valencak, T.G., Azzu, V. 2014. Making heads or tails of mitochondrial membranes in longevity
685 and aging: a role for comparative studies. *Longevity & Healthspan* **3**, 3
686 http://www.longevityandhealthspan.com/content/3/1/3

687 Velez, C. Figueira, E., Soarez, A.M.V.M., Freitas, R. 2017. Effects of seawater temperature
688 increase on economically relevant native and introduced clam species. *Mar. Env. Res.,* 123, 62-
689 70.

690 Ventrella, V., Pirini, M., Pagliarani, A., Trombetti, F., Manuzzi, M.P., Borgatti, A.R., 2008.
691 Effect of temporal and geographical factors on fatty acid composition of *M. galloprovincialis*
692 from the Adriatic sea. *Comp. Biochem. Physiol. B* 149, 241–250.

693 Ventrella, V., Pagliarani, A., Nesci, S., Trombetti, F., Pirini, M. 2013. Dietary enhancement of
694 selected fatty acid biosynthesis in the digestive gland of *Mytilus galloprovincialis* (Lmk). *J.*
695 *Agr. Food Chem*. 61, 973-981.

696 Wassall, S.R. and Stilwell, W. (2009). Polyunsaturated fatty acid-cholesterol interactions:
697 domain formation in membranes. *Biochim. Biophys. Acta* 1788, 24-32.

698 Zakhartsev, M.V., Naumenko, N.V., Chelomin, V.P. 1998. Non-methylene interrupted fatty
699 acids in phospholipids of the membranes of the mussel *Crenomytilus grayanus*. *Russian J. Mar.*
700 *Biol.* 24, 183-186.

701

Table 1. Fatty acid composition of clam gill mitochondria

Fatty acid	% (w/w)
14:0	0.7 ± 0.2
15:0+iso	0.6 ± 0.1
16:0	9.6 ± 0.3
16:1n-9	1.2 ± 0.1
16:1n-7	1.6 ± 0.3
17:0iso	0.6 ± 0.1
17:0	1.1 ± 0.2
16:3n-4	1.9 ± 0.4
18:0	7.1 ± 0.6
18:1n-9	2.9 ± 0.3
18:1n-7	1.3 ± 0.2
18:2n-6	0.9 ± 0.2
18:3n-3	3.2 ± 0.4
18:4n-3	2.0 ± 0.3
20:1n-11	1.7 ± 0.2
20:1n-9	0.8 ± 0.1
20:1n-7	0.7 ± 0.1
20:2Δ7,13	0.4 ± 0.1
20:2Δ7,15	2.0 ± 0.4
20:4n-6	5.2 ± 0.5
20:4n-3	4.2 ± 0.3
20:5n-3	8.1 ± 0.6
22:2Δ7,13	10.0 ± 0.4
22:2Δ7,15	2.4 ± 0.1
22:3n-6	2.6 ± 0.2
22:4n-6	0.9 ± 0.2
22:4n-3	2.3 ± 0.3
22:5n-3	3.0 ± 0.6
22:6n-3	22.1 ± 1.0
SFA	19.0 ± 1.5
MUFA	10.2 ± 0.6
PUFA	70.3 ± 1.0
NMI	14.8 ± 0.7
n–3	44.9 ± 2.1
n–6	9.6 ± 0.7
UI	16.4 ± 1.1

All values are the mean ± SE of 4 determinations carried out on different mitochondrial preparations. Cumulative and calculated parameters are in bold. Iso: branched fatty acid; SFA: saturated fatty acids; ,MUFA:monounsaturated fatty acids; PUFA: polyunsaturated fatty acids; NMI: non-methylene-interrupted fatty acids. The unsaturation index (UI) was calculated according to the formula: UI = [MUFA + dienoic fatty acids × 2 + trienoic fatty acids × 3 + tetraenoic fatty acids × 4 + pentaenoic fatty acids × 5 + esaenoic fatty acids × 6] / SFA.

736

737 Table 2. Gill mitochondrial sterols of Manila clams (*R. philippinarum*) and mussels (*M.*
738 *galloprovincialis)*°.
739

Sterol			Bivalves	
Common name	Systematic name§	Carbon atoms	Manila clam	Mussel
Stigmasterol	Stigmasta-5,22-dien-3β-ol	C_{29}	7.4±0.5	n.d.
β-sitosterol	Stigmast-5-en-3β-ol	C_{29}	0.9±0.2	n.d
Fucosterol	24-ethylidene-cholest-5-en-3β-ol	C_{29}	0.9±0.3	n.d.
Campesterol	Campest-5-en-3β-ol	C_{28}	2.2±0.2	n.d.
Brassicasterol	Ergosta-5,22-dien-3β-ol	C_{28}	9.2±1.0a	8.0±0.7a
24-Methylene-cholesterol	24-Methylene-cholest-5-en-3β-ol	C_{28}	13.9±2.5a	17.0±3.5a
Cholesterol	Cholest-5-en-3β-ol	C_{27}	42.1±2.0a	45.0±2.3a
Desmosterol	Cholest-5,24-dien-3β-ol	C_{27}	12.8±0.5a	21.0±1.0b
22-Dehydrocholesterol	Cholesta-5,22-dien-3β-ol	C_{27}	9.1±1.4a	6.0±0.8b
Occelasterol	27-Nor-24-methylcholesta-5,22-dien-3β-ol	C_{27}	n.d.	1.0±0.1
24-Norcholesta-5,22-diene-3β-ol	24-Norcholesta-5,22-dien-3β-ol	C_{26}	1.6±0.4a	2.0±0.1a

740

741 °to facilitate comparison between the two bivalve species, sterol percentages in mussel (*Mytilus*
742 *galloprovincialis*) gill mitochondria, obtained from Fiorini et al.(2016), were tabulated.
743 §Stereochemical assignments are omitted; n.d.: not detectable.
744 Values, evaluated on three distinct mitochondrial preparations for each species, are expressed
745 as percentage ± SD of total sterols. Within each row, different letters indicate significantly
746 different values ($P \leq 0.05$)
747
748

749 Table 3. Activation energies of the mitochondrial F_1F_O-ATPase in different species and tissues
750 at temperatures above (Ea_1) and below (Ea_2) the temperature of discontinuity (Td) of
751 the Arrhenius plot.
752

Species tissue	Ea_1 (Kcal/mole)	Td (°C)	Ea_2 (Kcal/mole)
Ruditapes philippinarum gills	8.9±1.1a	22.1±0.4a	23.1±1.3a
Mytilus galloprovincialis° gills	12.1±0.3b	20.1±0.2b	29.2±0.1b
Sus scrofa domesticus° heart	11.7±0.2b	21.8±0.3a	31.3±0.3c

753 Data are the mean ±SD of three replicate sets of experiments carried out on different
754 mitochondrial preparations. °To allow comparison, data from Fiorini et al (2016) were
755 tabulated. Within each column different letters indicate significantly different values ($P \leq 0.05$)
756

757

758 Table 4. Laurdan excitation GP values (Ex GP^{360}) detected at 10, 20, 30 °C in mitochondrial
759 membranes of *Ruditapes philippinarum* and *Mytylus galloprovincialis** gills and of
760 *Sus scrofa domesticus* heart* and in liposomes prepared from total lipid extracts of
761 mitochondria of these tissues

	Ex GP^{360}					
	Mitochondrial membranes			Liposomes		
assay temperature (°C)	*Ruditapes. philippinarun* gills	*Mytilus galloprovincialis* gills	*Sus scrofa domesticus* heart	*Ruditapes. philippinarun* gills	*Mytilus galloprovincialis* gills	*Sus scrofa domesticus* heart
10	0.45±0.02 a	0.32±0.02 a	0.35±0.03 a	0.46±0.01 a	0.47±0.01 a	0.35±0.03 a
20	0.36±0.02 b	0.32±0.01 a	0.27±0.03 b	0.34±0.02 b	0.44±0.02 a	0.24±0.02 b
30	0.27±0.02 c	0.31±0.02 a	0.21±0.02 c	0.29±0.01 c	0.40±0.01 c	0.15±0.03 c

762 Data are the mean ±SD of three determinations carried out on different animal pools. °To
763 allow comparison among the different tissues, data from Fiorini et al (2016) were tabulated.
764 Within each column different letters indicate significantly different values ($P \leq 0.05$)

765

766

767

768

769

770

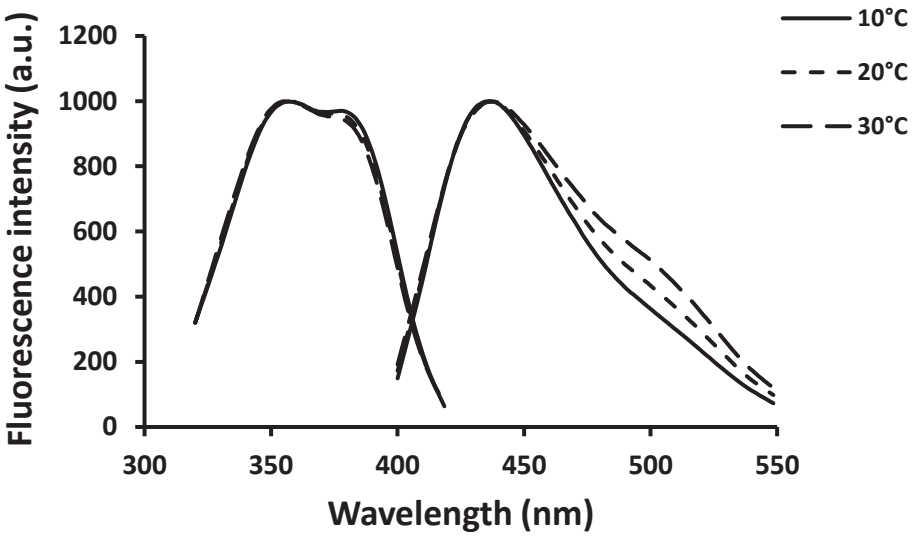

771

772 Fig. 1. Laurdan excitation and emission spectra in clam gill mitochondrial membranes.
773 Fluorescence measurements were carried out at 10° (solid line), 20° (dotted line), 30°C (dashed
774 line); (a.u., arbitrary units). Laurdan excitation and emission spectra were normalized by using
775 PerkinElmer FLWinLab Software. Each spectrum is the mean $\pm$ SD of three different
776 determinations performed on distinct animal pools. The SD (<0.05) are not shown for the clarity
777 of the spectra.

778

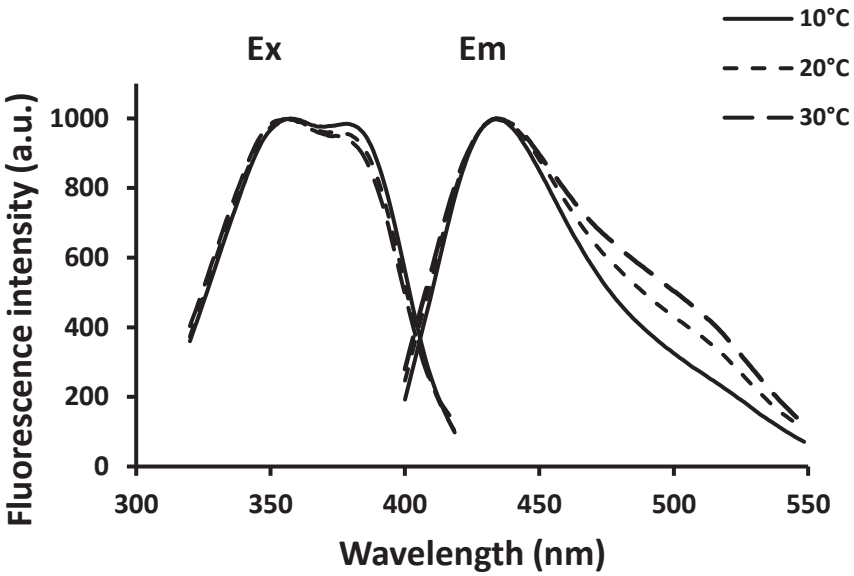

779

780 Fig. 2. Laurdan excitation and emission spectra in liposomes prepared from clam gill
781 mitochondrial lipids. Fluorescence measurements were carried out at 10° (solid line), 20°
782 (dotted line), 30°C (dashed line); (a.u., arbitrary units). Other conditions are as in Fig. 1.

783

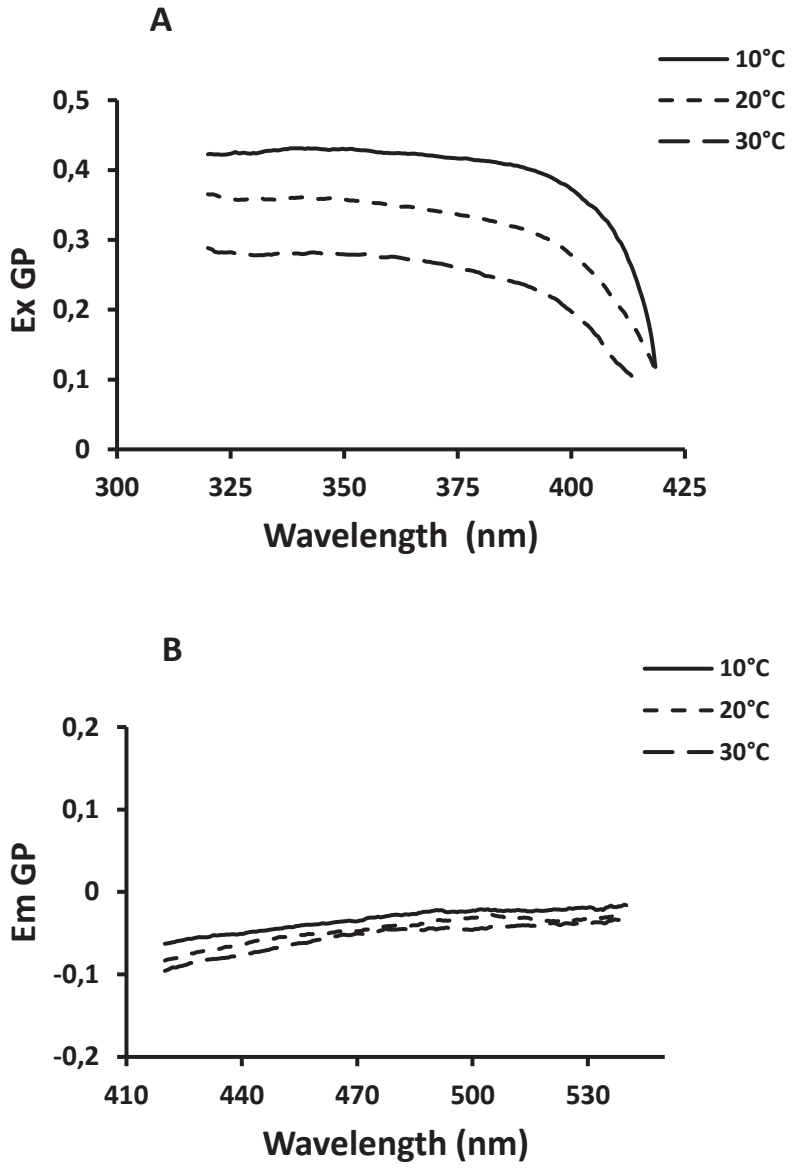

Fig. 3. Laurdan excitation (A) and emission (B) generalized polarization (GP) spectra in clam gill mitochondrial membranes. Fluorescence measurements were carried out at 10°(solid line), 20° (dotted line), 30°C (dashed line**),** respectively. (a.u., arbitrary units). Each spectrum is the mean ± SD of three different determinations performed on distinct animal pools. The excitation SD (<0.05) and the emission SD (>0.05 are not shown for the clarity of the spectra.

792

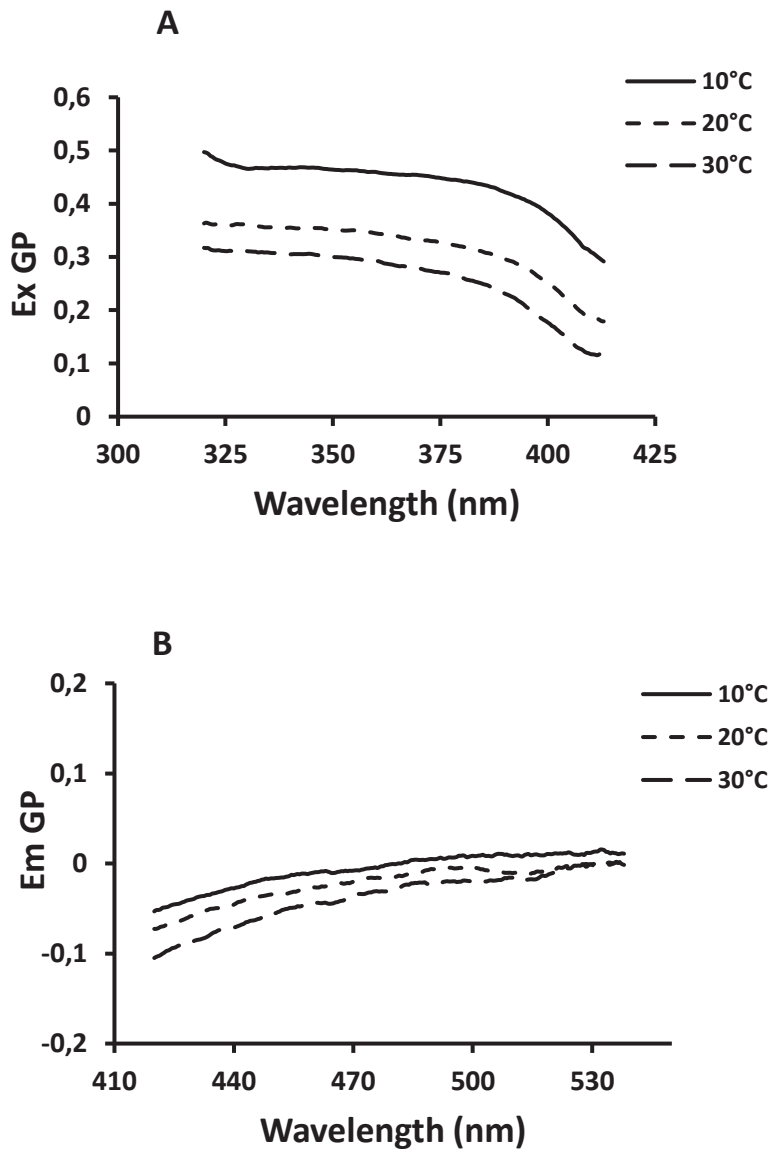

793

794

795 Fig.4. Laurdan excitation (A) and emission (B) generalized polarization (GP) spectra in
796 liposomes prepared from clam gill mitochondrial lipids**.** Fluorescence measurements were
797 carried out at 10° (solid line), 20° (dotted line), 30°C (dashed line), respectively**.** Each spectrum
798 is the mean ± SD of three different determinations performed on distinct animal pools. The SD
799 (<0.05) are not shown for the clarity of the spectra.

800